Multi-organ genetic causal connections inferred from imaging and clinical data through Mendelian randomization

Running title: MR atlas for multi-organ images

Juan Shu[1], Rong Zheng[2], Carlos Copana[1], Bingxuan Li[3], Zirui Fan[1,4], Xiaochen Yang[1], Yilin Yang[5], Xiyao Wang[3], Yujue Li[1], Bowei Xi[1], Tengfei Li[6,7], Hongtu Zhu[8,9,10,11]*, and Bingxin Zhao[1,4]*

[1]Department of Statistics, Purdue University, West Lafayette, IN 47907, USA.

[2]Department of Ultrasound Imaging, First Hospital of Shanxi Medical University, Taiyuan, Shanxi 030001, China.

[3]Department of Computer Science, Purdue University, West Lafayette, IN 47907, USA.

[4]Department of Statistics and Data Science, University of Pennsylvania, Philadelphia, PA 19104, USA.

[5]Department of Computer and Information Science and Electrical and Systems Engineering, School of Engineering & Applied Science, University of Pennsylvania, Philadelphia, PA 19104, USA.

[6]Department of Radiology, University of North Carolina at Chapel Hill, Chapel Hill, NC 27599, USA.

[7]Biomedical Research Imaging Center, School of Medicine, University of North Carolina at Chapel Hill, Chapel Hill, NC 27599, USA.

[8]Department of Biostatistics, University of North Carolina at Chapel Hill, Chapel Hill, NC 27599, USA.

[9]Department of Genetics, University of North Carolina at Chapel Hill, Chapel Hill, NC 27599, USA.

[10]Department of Computer Science, University of North Carolina at Chapel Hill, Chapel Hill, NC 27599, USA.

[11]Department of Statistics and Operations Research, University of North Carolina at Chapel Hill, Chapel Hill, NC 27599, USA.

**Corresponding authors*:

Hongtu Zhu

3105C McGavran-Greenberg Hall, 135 Dauer Drive, Chapel Hill, NC 27599.

E-mail address: htzhu@email.unc.edu Phone: (919) 966-7250

Bingxin Zhao

413 Academic Research Building, 265 South 37th Street, Philadelphia, PA 19104.

E-mail address: bxzhao@upenn.edu Phone: (215) 898-8222

Abstract

Functional and morphological architectures of major human organs have been well characterized using imaging biomarkers. Nevertheless, deciphering the causal relationships between imaging biomarkers and major clinical outcomes, as well as understanding the causal interplay across multiple organs, remains a formidable challenge. Mendelian randomization (MR) presents a framework for inferring causality by using genetic variants as instrumental variables. Here we report a systematic multi-organ MR analysis between 402 imaging biomarkers and 88 clinical outcomes. We identified 488 genetic causal links for 62 diseases and 130 imaging biomarkers from 9 organs, tissue, or systems, including the brain, heart, liver, kidney, lung, pancreas, spleen, adipose tissue, and skeleton system. We prioritized crucial intra-organ causal connections, such as the bidirectional genetic links between Alzheimer's disease and brain function, as well as inter-organ causal effects, such as the adverse impact of heart diseases on brain health. Our findings uncover the genetic causal links spanning multiple organs, offering a more profound understanding of the intricate relationships between organ imaging biomarkers and clinical outcomes.

Keywords: Brain imaging; Clinical outcomes; FinnGen; GWAS; Heart imaging; Mendelian randomization; MRI; Organ imaging; UK Biobank.

Medical images, such as magnetic resonance imaging (MRI), provide noninvasive assessments of the health of major human organs, such as the brain, heart, liver, and kidney. Imaging biomarkers have been widely used in clinical research and applications. For example, Alzheimer's disease-related abnormalities have been consistently observed in structural and functional imaging traits extracted from brain MRI, especially in the hippocampal region[1]. The cardiovascular MRI (CMR) provides reliable information on alterations in ventricular function, cardiovascular morphology, and myocardial perfusion, all of which are closely related to cardiovascular diseases[2]. Skeleton dual-energy X-ray absorptiometry (DXA) helps discover novel genetic variants which influence the human skeletal form and uncover a major evolutionary aspect of human anatomical change to pathogenesis[3]. Several large-scale organ imaging datasets (on the scale of over 10,000 participants) have recently been made publicly available, revealing details about human organ morphology and function[4-8]. A variety of complex traits and clinical outcomes are found to be associated with organ imaging biomarkers based on these well-powered population-based studies[9,10]. Despite these efforts, due to the inherent limitations of observational data, it remains challenging to definitively determine causal relationships between imaging biomarkers and clinical outcomes, as well as to fully understand the causal interconnections across multiple organs[11].

By using genetic variants as instrumental variables, Mendelian randomization (MR) can infer causality from observational data[12,13]. With assumptions regarding genetic, exposure, and outcome variables, MR aims to examine causal relationships between the exposure and the outcome variables while controlling for unwanted confounding factors. Family and population-based studies have shown that many imaging biomarkers and complex diseases are strongly influenced by genetics, with hundreds of associated genetic loci being identified in large-scale genome-wide association studies (GWAS)[8,14-29]. Leveraging these GWAS summary-level data (summary statistics), MR methods can uncover causality between imaging measurements and clinical endpoints. Several recent MR studies have examined the genetic causality of imaging biomarkers[11,30-35]. The major limitation of most of these MR studies has been focusing on one single organ (or imaging modality) and/or one single disease, or diseases in one single domain, such as brain imaging and psychiatric disorders[30]. It is known, however, that many diseases serve as the

causes and/or consequences of functional and structural changes in multiple organs of the human body. Cross-organ analysis aids in understanding the complexity of human physiology, subsequently enhancing our ability to diagnose, treat, and prevent a variety of diseases. Therefore, MR analysis from a multi-organ perspective is needed to uncover the clinical implications of imaging biomarkers in the context of the complex interplays of organ systems.

In this paper, we performed a systematic two-sample MR analysis of multi-organ images and clinical endpoints. We aggregated GWAS summary statistics from 402 multi-organ imaging biomarkers (average sample size $n \approx 35{,}000$) from the UK Biobank (UKB)[36] study and 88 clinical outcomes (number of cases > 10,000) collected by the FinnGen project[27] (**Fig. S1** and **Tables S1-S2)**. Specifically, we examined three major brain MRI modalities: 1) 101 regional brain volumes[21] from brain structural MRI (sMRI); 2) 110 diffusion tensor imaging (DTI) parameters[23] from brain diffusion MRI (dMRI); and 3) 90 functional activity (amplitude[37]) and connectivity traits from functional MRI (fMRI)[25]. In addition, we used 82 CMR traits extracted from short-axis, long-axis, and aortic cine cardiac MRI[38,39]. We also evaluated 11 abdominal MRI biomarkers, which gauged the volume, fat, or iron content in seven organs and tissues[8], as well as eight DXA imaging biomarkers that measured the lengths of all long bones and the width of the hip and shoulder[29]. The **Methods** section provides more details on these multi-organ imaging biomarkers. We applied 8 MR methods[40-48] to explore the bidirectional genetic causal links. The study design is presented in **Figure 1A** and a high-level summary of our findings can be found in **Figure 1B.**

RESULTS

Genetic causality between brain imaging and multi-organ diseases

In this section, we examined the causal relationship between brain imaging biomarkers and multi-organ diseases. At the Bonferroni significance level ($P < 5.18\times10^{-6}$, multiple testing adjustment for both directions), MR suggested 127 significant genetic causal effects on 58 brain imaging biomarkers from 20 diseases in 8 major categories, including mental and behavioral disorders, diseases of the nervous system, diseases of the circulatory system, cardiometabolic endpoints, interstitial lung disease endpoints,

diseases marked as autoimmune origin, diseases of the eye and adnexa, and diseases of the genitourinary system (**Fig. S2** and **Table S3**). Among all the diseases, heart-related diseases were the most frequent (66/127) and were predominantly associated with DTI parameters and a smaller number of regional brain volumes. No significant causal effects were observed from heart diseases to fMRI traits. The top three heart diseases that exhibited causal genetic impacts on brain structures included peripheral artery disease (15/66), hypertension (14/66), and hypertensive diseases (12/66) (**Figs. S2-S4**). For example, peripheral artery disease played a causal role in altering the white matter microstructure within the anterior limb of the internal capsule (ALIC, $|\beta|>0.15$, $P < 3.04\times10^{-8}$), the body of corpus callosum tract (BCC, $|\beta|>0.14$, $P < 8.44\times10^{-7}$), and the genu of corpus callosum tract (GCC, $|\beta|>0.13$, $P < 4.24\times10^{-6}$). Hypertension and hypertensive diseases were causally associated with the superior corona radiata (SCR, $|\beta|>0.07$, $P < 9.47\times10^{-8}$). In addition to DTI parameters, hypertension also negatively affected the total grey matter volume ($|\beta|>0.02$, $P < 1.26\times10^{-8}$) (**Figs. 2C** and **S2-S3**). In addition to heart-related diseases, several other non-neurological clinical endpoints also influenced brain health. For example, negative causal effects of asthma were found on the SCR ($|\beta|>0.05$, $P < 7.26\times10^{-7}$) and volume of the right inferior lateral ventricle ($|\beta|>0.09$, $P < 8.66\times10^{-7}$) (**Fig. S5**).

Brain disorders also causally affected the brain imaging biomarkers (49/127), with dementia and Alzheimer's disease being the most common brain-related diseases (**Fig. S2**). Interestingly, brain disorders were primarily associated with fMRI traits. For example, Alzheimer's disease was consistently found to be causally related to decreased functional activity in the dorsal attention ($|\beta|>0.04$, $P < 5.07\times10^{-8}$), frontoparietal, and secondary visual network ($|\beta|>0.04$, $P < 4.70\times10^{-8}$), as well as DTI parameters of the SCR ($|\beta|>0.03$, $P < 1.85\times10^{-6}$) (**Figs. 2A** and **S6**). Both functional MRI and DTI parameters have been extensively used to study Alzheimer's disease[49]. Abnormalities in white matter, such as those in the left SCR, as well as decreased functional connectivity in attention-related networks, have been identified in patients with Alzheimer's disease[50,51]. Similar to Alzheimer's disease, dementia demonstrated negative causal genetic effects on functional activity in multiple networks, including the cingulo-opercular, default mode, dorsal attention, frontoparietal, language, posterior multimodal, and secondary visual

networks ($|\beta|$>0.12, $P < 4.74\times10^{-8}$) (**Figs. 2B** and **S7**). In addition, mood disorders affected brain volume traits, such as the left and right putamen ($|\beta|$>0.04, $P < 5.64\times10^{-7}$) (**Fig. S8**). More results on causal genetic links from clinical endpoints to brain imaging traits were summarized in **Figures S3-S9**.

Brain and other organ diseases may also be caused by structural or functional changes in the brain. We investigated this direction by using brain imaging traits as exposure variables and clinical endpoints as the outcome variables. At the Bonferroni significance level ($P < 5.18\times10^{-6}$), we found 85 significant pairs between 22 brain imaging biomarkers and 20 clinical endpoints (**Fig. S10** and **Table S3**). Most of the significant imaging-disease pairs were related to fMRI traits. Specifically, 66 of the 85 pairs were associated with fMRI traits, 10 with DTI parameters, and 9 with regional brain volumes. The majority of the significant findings were related to brain diseases (65/85), with a minor proportion linked to heart diseases (13/85), autoimmune diseases (4/85), COPD and related endpoints (1/85), diseases of the eye and adnexa (1/85), and diseases of the genitourinary system (1/85). For example, decreased activity in multiple functional networks was related to a higher risk of Alzheimer's disease, such as the default mode and dorsal-attention networks ($|\beta|$>0.5, $P < 5.65\times10^{-13}$) (**Figs. 3A** and **S11**). We also identified genetic causal effects from DTI parameters on Alzheimer's disease, such as the BCC and SCR ($|\beta|$>0.49, $P < 6.79\times10^{-7}$) (**Figs. 3A** and **S11**).

Dementia exhibited a similar pattern to Alzheimer's disease, being causally influenced by decreased activity in multiple networks, such as the default mode, dorsal-attention, and secondary visual network ($|\beta|$>0.002, $P < 2.77\times10^{-7}$) (**Fig. 3B** and **S12**). fMRI traits, including the functional activity of the secondary visual network and functional connectivity of the default mode network, were also causally linked to other brain diseases, such as neuropsychiatric disorders ($|\beta|$>0.09, $P<8.88\times10^{-16}$) and neurological diseases ($|\beta|$>0.06, $P < 1.72\times10^{-6}$) (**Figs. S13** and **S14**). Finally, we found that brain structural alterations may also influence other non-neurological diseases. For example, the left basal forebrain posed a negative causal effect on hypertensive diseases ($|\beta|$>0.12, $P < 8.47\times10^{-9}$) and hypertension ($|\beta|$>0.15, $P < 6.19\times10^{-11}$). The left lingual negatively affected female genital prolapse ($|\beta|$>0.75, $P < 8.68\times10^{-7}$).

Causal genetic relationships between CMR traits and clinical outcomes

We first examined the causal effects from clinical endpoints to CMR measures of heart structure and function. We identified 111 significant results at the Bonferroni significance level ($P < 6.85\times10^{-6}$), covering 41 unique CMR traits of the ascending aorta (AAo), descending aorta (DAo), left atrium (LA), and left ventricle (LV). Significant causal effects were found from 13 unique clinical endpoints in three categories: diseases of the circulatory system (8/13), cardiometabolic endpoints (4/13), as well as COPD and related endpoints (1/13). The majority of significant findings were related to heart-related diseases, with 66 out of 111 being diseases of the circulatory system and 44 out of 111 being cardiometabolic endpoints (**Fig. S15** and **Table S4**).

The most frequently observed genetic effects were related to hypertensive diseases and hypertension (**Figs. 4A** and **S16**). Specifically, hypertensive diseases had negative causal effects on AAo and DAo distensibility ($|\beta|>0.10$, $P < 1.26\times10^{-7}$), whose genetic associations have been found in previous studies[52-54]. Hypertensive diseases also affected LV and LA traits, such as the global radial strain ($|\beta|>0.06$, $P < 4.47\times10^{-9}$), LA stroke volume ($|\beta|>0.07$, $P < 3.04\times10^{-8}$), and LV myocardial mass ($|\beta|>0.11$, $P < 3.04\times10^{-15}$). These findings were consistent with previous results derived from genetic association studies[55,56]. Hypertension exhibited a similar pattern to hypertensive diseases, having a causal impact on various AAo and DAo traits, such as DAo distensibility, along with LA and LV traits, such as the LA minimum volume (LA_{min} volume, $|\beta|>0.03$, $P < 7.11\times10^{-6}$).

In addition, angina pectoris causally influenced AAo maximum and minimum areas (AAo_{max} and AAo_{min} areas, $|\beta|>0.71$, $P < 1.44\times10^{-7}$). The aortic aneurysm had a positive causal effect on DAo maximum and minimum areas (DAo_{max} and DAo_{min} areas, $|\beta|>0.71$, $P < 1.63\times10^{-24}$) and AAo_{max} and AAo_{min} areas ($|\beta|>0.16$, $P < 2.22\times10^{-6}$). These results align with clinical observations. Atrial fibrillation and flutter mainly affected LA traits, such as the LA ejection fraction ($|\beta|>0.07$, $P < 5.88\times10^{-8}$), LA maximum volume (LA_{max} volume, $|\beta|>0.07$, $P < 1.62\times10^{-6}$), and LA_{min} volume ($|\beta|>0.08$, $P < 8.26\times10^{-8}$). Atrial fibrillation is considered to result in a decrease in ejection fraction as well as an increase in LA volumes[57,58]. In addition to heart-related diseases, COPD and related endpoints were

found to influence CMR traits, such as the negative effect of COPD on DAo_{max} area ($|\beta|>0.10$, $P < 4.45\times10^{-11}$, and **Fig. S16**). Emphysema, a form of COPD distinguished by the degradation of lung tissue, may contribute to the dilatation of the thoracic aorta[59]. This could be attributed to emphysema's involvement in the degradation of elastic fibers within the lungs, potentially triggering alterations in the aortic wall's elasticity[60]. Such changes may precipitate the dilatation or ballooning of the thoracic aorta, thereby escalating the risk of both aortic aneurysm and abdominal aortic abnormalities[59]. This elucidates the potential biological mechanisms driving these causal relationships.

On the other hand, structural and functional irregularities of the heart may increase the risk of multi-organ diseases, given that the heart pumps blood to all other organs to maintain their functions[61]. We tested this direction by treating CMR traits as exposure variables and clinical endpoints as the outcomes. After Bonferroni adjustment ($P < 6.85\times10^{-6}$), we found 27 significant causal pairs, 25 for heart-related diseases and 2 for autoimmune diseases (**Fig. S17** and **Table S4**). For example, global peak circumferential strain was positively linked to heart failure and antihypertensive medication ($|\beta|>0.51$, $P < 8.49\times10^{-8}$), while LV ejection fraction had a negative causal effect on these conditions ($|\beta|>0.55$, $P < 1.12\times10^{-6}$). In addition to heart-related diseases, heart structural changes affected diseases marked as autoimmune origin. For example, right ventricular end-systolic volume had a negative causal effect on the autoimmune diseases defined by Finngen[27] ($|\beta|>0.18$, $P < 3.10\times10^{-6}$) (**Figs. 4B** and **S18**). In summary, we discovered causal relationships between CMR traits and heart-related diseases, which were typically bidirectional. Additionally, we revealed the inter-organ causal relationships between the heart and other organs.

Causal genetic links between abdominal imaging biomarkers and clinical outcomes

We first examined the effects of multi-organ diseases on abdominal imaging biomarkers, such as the volume or iron content of the spleen, kidney, liver, lung, and pancreas[8]. At the Bonferroni significance level ($P < 6.69\times10^{-5}$), we discovered 51 significant causal pairs from multi-organ diseases to abdominal imaging biomarkers, with liver imaging traits being the most impacted (26/51). Brain-related diseases were the most prevalent among all significant findings (35/51), followed by heart-related diseases (7/51), rheumatoid

endpoints (4/51), diseases of the eye and adnexa (3/51), and autoimmune diseases (2/51) (**Fig. S19** and **Table S5**). These findings were in line with ongoing research on the interplay between the brain and abdominal organs, such as the brain-gut connection[62-64], brain-kidney connection[65,66], and brain-liver connection[67].

Alzheimer's disease and dementia were consistently found to be causally linked with various abdominal imaging biomarkers, such as the percent liver fat ($|\beta|>0.37$, $P < 4.96\times10^{-6}$), liver volume ($|\beta|>0.03$, $P < 5.88\times10^{-5}$), and adipose tissue measurement ($|\beta|>0.06$, $P < 3.13\times10^{-5}$). In addition to Alzheimer's disease and dementia, there were multiple other brain-related diseases that may affect abdominal organs, including mental and behavioral disorders due to alcohol and psychoactive substance use, as well as sleep apnoea. For example, sleep apnoea influenced several abdominal traits, such as the liver volume ($|\beta|>0.11$, $P < 2.80\times10^{-5}$) and kidney volume ($|\beta|>0.23$, $P < 2.57\times10^{-6}$). Sleep apnea can lead to renal damage caused by ischemic stress, hemodynamic changes, or intermediary conditions such as hypertension, which can result in early chronic kidney disease[68,69]. Multiple heart-related diseases also genetically impacted abdominal organs. For example, heart failure and antihypertensive medication can lead to larger spleen volume ($|\beta|>0.004$, $P < 2.66\times10^{-6}$). It has been found that heart splenic enlargement often results from blood stasis and right heart disease is often accompanied by splenomegaly[70]. Atherosclerosis was causally linked to the pancreas iron content, which was also supported by clinical evidence[71,72].

In addition to brain and heart-related diseases, we also observed causal effects from other diseases, such as autoimmune diseases on spleen volume and liver iron content. The spleen, as the largest immune organ in the body, can become enlarged because of various rheumatic and immune system diseases, such as systemic lupus erythematosus, Felty's syndrome, sarcoidosis, and autoimmune hepatitis[73-76]. Liver iron content causally related to both autoimmune and rheumatological diseases ($|\beta|>0.10$, $P < 3.02\times10^{-5}$). It has been found that excessive deposition of iron ions exists in the affected tissues of autoimmune diseases, such as brain tissues of multiple sclerosis patients and synovial fluid of patients with rheumatoid arthritis[77]. Disorders of the choroid and retina, as well as the eye and adnexa diseases, were also found to be causally linked to liver iron content

(|β|>0.10, $P < 6.48\times10^{-5}$, **Figs. 5A** and **S20**). Metal tends to accumulate in human ocular tissues, particularly in the choroid and retinal pigment epithelium[78].

Next, we tested the opposite direction that abdominal imaging biomarkers being the exposure variables and multi-organ diseases being the outcomes. At the Bonferroni significance level ($P < 6.69\times10^{-5}$), we identified 55 significant pairs, with heart-related diseases being the most prevalent (34/55), followed by brain-related diseases (11/55), diseases marked as autoimmune origin (2/55), diseases of the eye and adnexa (5/55), and diseases of the genitourinary system (3/55) (**Fig. S21** and **Table S5**). For example, pancreas fat causally affected the deep vein thrombosis of lower extremities and pulmonary embolism (|β|>0.38, $P < 1.04\times10^{-12}$). A reduction in pancreatic fat content may directly improve cellular function and insulin secretion rate, affecting triglyceride levels and blood flow[79].

Larger liver, spleen, and kidney volumes were all causally linked to heart-related diseases (**Fig. 5B** and **S22**). Specifically, a larger liver volume was causally linked to hypertensive diseases and hypertension (|β|>0.13, $P < 1.19\times10^{-10}$); a larger kidney volume was causally related to a higher risk of stroke (|β|>0.25, $P < 3.33\times10^{-5}$); and a larger spleen volume had causal effects on various heart-related diseases, including coronary angioplasty (|β|>0.14, $P < 4.94\times10^{-7}$), coronary atherosclerosis (|β|>0.07, $P < 6.94\times10^{-10}$), and peripheral artery diseases (|β|>0.21, $P < 4.98\times10^{-5}$). In nephrotic syndrome, platelet over-activation and the use of diuretics and glucocorticoids can aggravate hypercoagulability. Therefore, kidney diseases, especially nephrotic syndrome, are prone to thrombotic and embolic complications, which can lead to stroke[80-82]. For brain-related disorders, we detected causal effects from liver volume to alcohol use disorder, as well as mental and behavioral disorders due to alcohol and psychoactive substance use. In addition, percent liver fat had causal links with Alzheimer's disease, dementia, and psychiatric diseases. Previous studies have reported that non-alcoholic fatty liver disease contributes to neurological conditions like cognitive impairment and memory loss via insulin resistance and inflammation, along with excessive cytokine secretion[83-86]. In summary, we found that brain-related disorders result in alterations in abdominal organs. Furthermore, bidirectional relationships are observed in both neurodegenerative and psychiatric

disorders. On the other hand, multiple abdominal organs are causally linked to heart-related diseases.

Causal genetic links between skeleton DXA traits and clinical outcomes

We first identified the causal effects of multiple organ diseases on DXA-derived skeleton traits[3]. At the Bonferroni significance level ($P < 3.39\times10^{-5}$), we found strong evidence that multi-organ diseases affected the human skeleton health, where heart-related diseases (6/12) and diseases of the nervous system (4/12) were the majority, as well as rheumatic disease (1/12) and diseases of the genitourinary system (1/12) (**Fig. S23** and **Table S6**). Carpal tunnel syndrome ($|\beta|>0.0007$, $P < 6.25\times10^{-8}$) and sleep apnoea ($|\beta|>0.001$, $P < 6.35\times10^{-8}$) were causally related to higher average forearm length. Carpal tunnel syndrome is when the median nerve (nerve from the forearm to the palm of the hand) becomes pressed or squeezed, which affects the wrist-to-forearm ratio[87,88]. It has been observed that oral appliance therapy[89], which is an effective treatment of sleep apnea, is associated with skeletal changes[90]. Furthermore, the nerve, nerve root, and plexus disorders were causally linked with higher average tibia length ($|\beta|>0.001$, $P < 2.78\times10^{-5}$), which was consistent with the previous finding that a specific type of plexus disorder, lumbosacral plexus disorder, is associated with lower leg[91]. Heart-related diseases also had causal effects on several DXA traits. For example, coronary heart disease had a negative causal effect on the average tibia length ($|\beta|>0.0002$, $P < 2.50\times10^{-5}$) and a positive causal effect on the hip width ($|\beta|>0.0004$, $P < 1.68\times10^{-5}$). Additionally, gonarthrosis affected the average tibia length ($|\beta|>0.0005$, $P < 1.69\times10^{-5}$) (**Figs. 6A** and **S24**).

The skeletal system serves as the foundational support for the human body, and therefore, skeletal abnormalities may potentially contribute to risk of multi-organ diseases. We identified 17 causal pairs at the Bonferroni significance level ($P < 3.39\times10^{-5}$). More than half (10/17) of these results were related to the heart, and the rest were rheumatic disease (3/17), diseases of the eye and adnexa (2/17), interstitial lung diseases (1/17), and diseases of the genitourinary system (1/17) (**Fig. S23** and **Table S6**). Average tibia length was causally linked to coxarthrosis ($|\beta|>30.03$, $P < 3.11\times10^{-9}$), gonarthrosis ($|\beta|>19.39$, $P < 3.18\times10^{-7}$), and other rheumatological endpoints ($|\beta|>13.12$, $P < 2.74\times10^{-5}$). It has been

found that the leg length discrepancy could lead to lower limb biomechanics, such as gonarthrosis, coxarthrosis, and other lower limb symptoms[92,93]. Torso length causally affected heart-related issues, such as coronary angioplasty ($|\beta|$>38.85, $P < 9.45\times10^{-5}$), coronary atherosclerosis ($|\beta|$>22.94, $P < 1.22\times10^{-5}$), hard cardiovascular diseases ($|\beta|$>18.12, $P<1.30\times10^{-5}$), and ischemic heart diseases ($|\beta|$>30.99, $P < 1.33\times10^{-5}$). Previous studies examining the relationship between skeletal length and heart diseases have primarily focused on leg length or overall body height, generally reporting negative associations[94,95]. Consistent with these associations, we found that a long torso can lead to a higher risk of heart disease. We also observed higher average tibia length to be causally linked to a lower risk of hypertension ($|\beta|$>6.46, $P < 1.27\times10^{-7}$), which was in line with previous findings[96] (**Figs. 6B** and **S25**). In conclusion, we found that rheumatoid endpoints (such as gonarthrosis) and diseases of the nervous system (such as nerve, nerve root, and plexus disorders) had a significant impact on bone health. Conversely, skeletal traits, like torso length, demonstrated a causal link with heart diseases.

Discussion

Observational studies have established numerous links between various imaging-derived phenotypes and clinical outcomes. However, these associations are frequently influenced by residual confounding, complicating the accurate inference of causal effect sizes [97]. MR allows for the inference of causal relationships between exposure and outcome variables. MR leverages the natural and random assortment of genetic variants during meiosis, making these variants an ideal choice as instrumental variables to discern causal effects. In the present study, we evaluated the causal relationship between 402 multi-organ imaging biomarkers and 88 clinical outcomes through bidirectional MR. To avoid the issue of sample overlap[98], which may bias the causal effect and has sometimes been overlooked in many current MR-based studies, we used a two-sample MR design and sourced our imaging and clinical data from different large-scale cohorts.

It is widely understood that diseases often affect more than just one part of the human body, given the interdependent nature of our organ systems for overall body function. The brain and heart are particularly important among all organs, as the brain manages a range of functions, including reactions, emotions, vision, memory, and cognition[99,100]

while the heart serves as the engine of the body, pumping life-sustaining blood through a network of arteries and veins to supply other organs with the oxygen and nutrients they need. Dysfunctions in various organs can potentially have adverse effects on the brain and heart. Similarly, abnormalities within the brain and heart can result in dysfunction in other parts of the body. Our results support the presence of robust bidirectional interactions between the brain and heart with other organs. In addition to the connections to the brain and heart, we also discovered many other causal relationships for other organs. The interaction plot across different organ systems can be found in **Figure 1B**. Below we provide more detailed discussions of these specific findings.

Intra-brain causal connections.

Variations in brain structure and function were closely linked with brain disorders, with parts of these relationships appearing to be bidirectional. We consistently found causal links between brain imaging biomarkers and multiple psychiatric disorders or neurological diseases, such as Alzheimer's disease, dementia, mood disorder, and sleep apnea. For example, Alzheimer's disease and dementia had bidirectional causal links with fMRI traits and DTI parameters. Previous studies have consistently shown that resting fMRI connectivity patterns are altered in patients with Alzheimer's disease[101,102], especially in brain regions involved in memory and cognitive function[103,104].

Brain-heart causal connections.

While association studies have been investigating the brain-heart interaction[39,105], the causal genetic links within these heart-brain systems remain largely unexplored. We discovered causal connections from several heart-related diseases such as hypertension, hypertensive diseases, heart failure, and peripheral artery disease to DTI parameters in white matter tracts such as the SCR, ALIC, BCC, GCC, the splenium of corpus callosum, and the retrolenticular part of the internal capsule (RLIC). Additionally, these diseases were also linked to regional brain volumes, such as grey matter and left amygdala. Hypertension can lead to damage of the blood vessels in the brain[106], which can in turn lead to a reduction in the volume of grey matter in certain brain regions[107]. This may result in cognitive impairment and an increased risk of developing dementia. Therefore, effective management of hypertension through lifestyle changes and medication can help

reduce the risk of these negative effects on the brain. On the other hand, alterations in brain structure, such as deformations in the left ventral DC and left basal forebrain, were found to contribute to heart-related diseases like hypertension. Similarly, changes in the left superior temporal region were linked to heart failure. These could be attributed to the brain's essential function in controlling blood pressure via a sophisticated network that involves multiple regions and pathways[108,109].

Bidirectional connections between the brain and abdominal organs.

Brain abnormalities affected multiple abdominal organs and the skeletal system. For example, Alzheimer's disease and dementia causally affected the percent liver fat, and neurological diseases (defined by FinnGen[27]) had a positive causal effect on lung volume. It has been found that neurological diseases, such as multiple sclerosis, Parkinson's disease, amyotrophic lateral sclerosis, and Huntington's disease, can cause respiratory muscle weakness[110,111], which can affect lung volume and function. We also found sleep apnoea may lead to larger spleen and kidney volume. This may be due to the increased workload on the spleen to filter blood and remove damaged red blood cells. Additionally, the low oxygen levels associated with sleep apnea can lead to an increase in the number of red blood cells in the body, which can also contribute to splenomegaly and a change in kidney volume. Sleep apnea was causally associated with increased pancreas iron content, potentially due to the decreased oxygen levels that accompany sleep apnea, resulting in increased iron absorption in the body. The excess iron in the pancreas can lead to oxidative stress and inflammation[112,113], which can contribute to the development of pancreatic damage and dysfunction[114-116].

In addition to the aforementioned neurological diseases, we also discovered that mental and behavioral disorders attributed to alcohol can lead to an increase in percent liver fat. It has been found that people with alcohol use disorder are more likely to develop alcoholic fatty liver disease[117]. Besides brain-related diseases, brain structural alternations could also lead to a higher risk of diseases of other organs. For example, right postcentral was causally linked to COPD. Some studies have suggested that chronic stress and anxiety, which are associated with changes in brain structure, may contribute to the development or worsening of respiratory conditions such as COPD[118,119].

On the other hand, brain imaging biomarkers or disorders were causally affected by several diseases of other organs or systems. A high percent liver fat resulted in a lower risk of Alzheimer's disease and dementia. Previous studies[120,121] have reported associations between the two and our results aligned with the most recent study[122]. More work is needed to understand the underlying pathophysiological mechanism. Brain imaging biomarkers were affected by multi-organ diseases, but some of them may affect the brain indirectly, such as through mediating effects of anxiety and depression. For example, diseases of the genitourinary system (ovarian cyst and menorrhagia) causally affected brain structural features. Ovarian cysts can cause hormonal imbalances due to the production of hormones by the cysts themselves[123]. These hormonal imbalances can cause a range of symptoms, such as mood swings, anxiety, and depression[124], which can affect brain function and emotional regulation. Diseases of the eye and adnexa (conjunctivitis) had genetic causal effects on functional connectivity traits. Conjunctivitis can be caused by a viral or bacterial infection, which can potentially lead to cause systemic inflammation in the body[125]. Systemic inflammation has been linked to changes in brain function and structure and may affect brain fMRI traits[126,127].

In addition, asthma influenced regional brain volumes. One prevalent way in which asthma impacts the brain is via the emotional and psychological stress associated with managing a chronic illness. Anxiety, stress, and depression, often faced by individuals with asthma, can induce alterations in brain structure. Previous studies have shown that individuals with asthma may have reduced cognitive function, including impaired memory and attention, and changes in brain activity patterns during cognitive tasks[128,129]. Last but not least, autoimmune diseases (defined by FinnGen[27]) affected brain imaging biomarkers, such as DTI parameters of the RLIC and SCR. Multiple sclerosis is an autoimmune disease that affects the central nervous system, and the damage to the myelin sheath that surrounds axons can occur in various regions of the brain[130,131], including the internal capsule. The damage can cause disruptions in the neural connections passing through the anterior limb, leading to symptoms such as weakness, spasticity, and difficulty with balance and coordination. In some rare autoimmune diseases, such as neuromyelitis optica[132] and autoimmune encephalitis, inflammation and damage can occur in the brain.

The resulting neurological symptoms can vary depending on the severity and location of the damage[133,134]. Furthermore, autoimmune diseases that cause systemic inflammation, such as rheumatoid arthritis and lupus, which can potentially affect the brain[135] and white matter tracts[136,137]. Chronic inflammation can lead to changes in the microstructure of white matter tracts, which can result in alterations in neural connectivity and function[138,139].

Intra-heart causal connections.

Bidirectional causal relationships were identified between heart-related diseases and CMR traits. Hypertension and hypertensive diseases were found to causally influence several CMR traits across various heart chambers and aorta regions. Conversely, variations in CMR traits were observed to potentially lead to heart diseases. These findings are in accordance with existing clinical evidence. For example, hypertension can cause the LA to enlarge, a condition known as left atrial hypertrophy[140,141]. This enlargement can lead to several complications, including atrial fibrillation, heart failure, and stroke[142]. As for atrial fibrillation, the electrical signals that control the heartbeat become chaotic, causing the heart to beat irregularly and often too fast. Over time, the constant irregularity of the heartbeat can also cause the LA to enlarge and weaken[143].

Bidirectional connections between the heart and abdominal organs.

Heart diseases and various multi-organ imaging biomarkers were causally related. For instance, heart failure was found to cause an increase in spleen volume. When the heart is not able to pump blood effectively, it can cause an increase in the pressure from the veins to the spleen. This increased pressure can cause the spleen to enlarge, a condition known as splenomegaly[144]. In addition, the backup of blood in the liver that can occur with heart failure can also contribute to the development of splenomegaly. Larger spleen volume can conversely lead to heart failure. An enlarged spleen can increase the workload on the heart, leading to further worsening of heart failure symptoms.

Pancreas was also found to have a causal effect on the heart. For example, excess pancreas fat was found to cause a higher risk of developing deep vein thrombosis of lower extremities and pulmonary embolism. Pancreatic steatosis is a condition where fat

accumulates in the pancreas. This is associated with a number of metabolic abnormalities, including insulin resistance and inflammation, which can contribute to the development of cardiovascular disease[145,146]. The inflammatory and procoagulant effects of excess pancreatic fat could potentially contribute to an increased risk of deep vein thrombosis.

The heart and lungs are closely connected and work together as part of the cardiovascular system. The lungs are responsible for taking in oxygen from the air we breathe and transferring it into the bloodstream, while the heart pumps the oxygen-rich blood throughout the body to nourish cells and tissues. We found strong evidence of causal links from COPD and CMR traits of DAo. The degradation of elastic fibers through proteolysis is a characteristic of emphysema[147], which can potentially lead to the enlargement of the thoracic aorta.

Spleen, as the largest immune organ, is closely related with diseases marked as autoimmune origin. We found strong evidence showing the genetic causal relationship between spleen volume and autoimmune diseases (defined by Finngen[27]), such as rheumatoid arthritis, systemic lupus erythematosus, and systemic sclerosis. It has been reported that autoimmune diseases can affect the spleen. For instance, conditions like lupus or rheumatoid arthritis can lead to splenomegaly, a condition often triggered by inflammation or the accumulation of abnormal immune cells in the spleen[148,149].

Skeleton DXA traits.

We also found genetic causal links between skeleton DXA traits and multiple organ diseases. Skeleton traits were causally affected by diseases of the nervous system, rheumatic disease, as well as nerve, nerve root and plexus disorders. Heart diseases may also impact the skeletal system by influencing bone health. It has been observed that individuals with heart disease, especially those with heart failure, have an increased risk of osteoporosis and bone fractures[149,150]. This may be due to a variety of factors. For example, some medications used to treat heart diseases, such as diuretics and steroids, can also increase the risk of osteoporosis[151]. Additionally, individuals with heart disease may have reduced mobility and physical activity, which can lead to decreased bone density and strength[152]. Skeleton problems could also inversely contribute to numerous

organ diseases, with heart conditions being the most prevalent in our analysis. A long torso may lead to a high risk of coronary heart disease. We also noted that a higher average tibia length was causally associated with a lower risk of hypertension, a finding that aligns with clinical observations[96].

Limitations and conclusions.

Our study has several limitations. First, we collected GWAS summary statistics from publicly available databases, meaning that we were not able to evaluate the impact of unobserved confounders (such as population stratification) on our results. Second, one common limitation of most existing MR methods is that they require several model assumptions, and thus may suffer from model misspecifications and data heterogeneity issues when integrating data from different data resources[153]. We have systematically applied quality control measures and conducted sensitivity analyses in our study. Future research implementing more advanced MR methods may relax some of the model assumptions the current MR methods have made[154,155]. Furthermore, MR studies are designed to examine the effects of lifetime exposure factors on outcomes, not interventions within a specified period. As such, our findings may have different interpretations from rigorous results obtained from randomized controlled trials. Therefore, any clinical interventions based on these MR findings should be undertaken with caution.

In conclusion, we used two-sample bidirectional MR analyses to comprehensively explore the multi-organ causal connections between 88 clinical outcomes and 402 image-derived phenotypes of various organ systems. Our results revealed robust genetic evidence supporting causal connections within and across multiple organs. This will aid in unraveling complex pathogenic mechanisms and will contribute to the early prediction and prevention of multi-organ diseases from a whole body perspective.

METHODS

Methods are available in the ***Methods*** section.

Note: One supplementary pdf file and one supplementary table zip file are available.

ACKNOWLEDGEMENTS

The study has been partially supported by funding from the Wharton Dean's Research Fund and Analytics at Wharton, as well as start-up funds from Purdue Statistics Department. This research has been conducted using summary-level data from the UK Biobank study and FinnGen research project. We would like to thank the individuals who represented themselves in the UK Biobank and FinnGen studies for their participation and the research teams for their efforts in collecting, processing, and disseminating these datasets. We would like to thank the research computing groups at the University of North Carolina at Chapel Hill, Purdue University, and the Wharton School of the University of Pennsylvania for providing computational resources and support that have contributed to these research results.

AUTHOR CONTRIBUTIONS

J.S. and B.Z. designed the study. J.S., R.Z., C.C., B.L., Z. F., X.Y., Y.Y, X.W., and Y.L. analyzed the data. B.X., T.L., and H.Z. provided feedback on the results. J.S. and B.Z. wrote the manuscript with feedback from all authors.

CORRESPONDENCE AND REQUESTS FOR MATERIALS should be addressed to H.Z. and B.Z.

COMPETING FINANCIAL INTERESTS

The authors declare no competing financial interests.

REFERENCES

1. Buckner, R.L.*, et al.* Molecular, structural, and functional characterization of Alzheimer's disease: evidence for a relationship between default activity, amyloid, and memory. *Journal of neuroscience* **25**, 7709-7717 (2005).
2. Pennell, D.J.*, et al.* Clinical indications for cardiovascular magnetic resonance (CMR): Consensus Panel report. *European heart journal* **25**, 1940-1965 (2004).
3. Kun, E.*, et al.* The genetic architecture of the human skeletal form. *bioRxiv*, 2023.2001. 2003.521284 (2023).
4. Petersen, S.E.*, et al.* UK Biobank's cardiovascular magnetic resonance protocol. *Journal of cardiovascular magnetic resonance* **18**, 1-7 (2015).

5. Littlejohns, T.J., Sudlow, C., Allen, N.E. & Collins, R. UK Biobank: opportunities for cardiovascular research. *European heart journal* **40**, 1158-1166 (2019).
6. Miller, K.L*., et al.* Multimodal population brain imaging in the UK Biobank prospective epidemiological study. *Nature Neuroscience* **19**, 1523-1536 (2016).
7. Thompson, P.M*., et al.* ENIGMA and global neuroscience: A decade of large-scale studies of the brain in health and disease across more than 40 countries. *Translational psychiatry* **10**, 1-28 (2020).
8. Liu, Y*., et al.* Genetic architecture of 11 organ traits derived from abdominal MRI using deep learning. *Elife* **10**, e65554 (2021).
9. Smith, S.M. & Nichols, T.E. Statistical challenges in "big data" human neuroimaging. *Neuron* **97**, 263-268 (2018).
10. Tian, Y.E*., et al.* Heterogeneous aging across multiple organ systems and prediction of chronic disease and mortality. *Nature Medicine*, 1-11 (2023).
11. Taschler, B., Smith, S.M. & Nichols, T.E. Causal inference on neuroimaging data with Mendelian randomisation. *NeuroImage*, 119385 (2022).
12. Sanderson, E*., et al.* Mendelian randomization. *Nature Reviews Methods Primers* **2**, 1-21 (2022).
13. Pingault, J.-B*., et al.* Using genetic data to strengthen causal inference in observational research. *Nature Reviews Genetics* **19**, 566-580 (2018).
14. Aung, N*., et al.* Genome-wide analysis of left ventricular image-derived phenotypes identifies fourteen loci associated with cardiac morphogenesis and heart failure development. *Circulation* **140**, 1318-1330 (2019).
15. Córdova-Palomera, A*., et al.* Cardiac Imaging of Aortic Valve Area From 34 287 UK Biobank Participants Reveals Novel Genetic Associations and Shared Genetic Comorbidity With Multiple Disease Phenotypes. *Circulation: Genomic and Precision Medicine* **13**, e003014 (2020).
16. Meyer, H.V*., et al.* Genetic and functional insights into the fractal structure of the heart. *Nature* **584**, 589-594 (2020).
17. Pirruccello, J.P*., et al.* Analysis of cardiac magnetic resonance imaging in 36,000 individuals yields genetic insights into dilated cardiomyopathy. *Nature communications* **11**, 1-10 (2020).

18. Pirruccello, J.P., *et al.* Genetic Analysis of Right Heart Structure and Function in 40,000 People. *bioRxiv* (2021).
19. Thanaj, M., *et al.* Genetic and environmental determinants of diastolic heart function. *medRxiv* (2021).
20. Elliott, L.T., *et al.* Genome-wide association studies of brain imaging phenotypes in UK Biobank. *Nature* **562**, 210-216 (2018).
21. Zhao, B., *et al.* Genome-wide association analysis of 19,629 individuals identifies variants influencing regional brain volumes and refines their genetic co-architecture with cognitive and mental health traits. *Nature genetics* **51**, 1637-1644 (2019).
22. Smith, S.M., *et al.* An expanded set of genome-wide association studies of brain imaging phenotypes in UK Biobank. *Nature neuroscience* **24**, 737-745 (2021).
23. Zhao, B., *et al.* Common genetic variation influencing human white matter microstructure. *Science* **372**, eabf3736 (2021).
24. Grasby, K.L., *et al.* The genetic architecture of the human cerebral cortex. *Science* **367**, eaay6690 (2020).
25. Zhao, B., *et al.* Genetic influences on the intrinsic and extrinsic functional organizations of the cerebral cortex. *medRxiv*, 2021.2007. 2027.21261187 (2021).
26. Watanabe, K., *et al.* A global overview of pleiotropy and genetic architecture in complex traits. *Nature genetics* **51**, 1339-1348 (2019).
27. Kurki, M.I., *et al.* FinnGen: Unique genetic insights from combining isolated population and national health register data. *medRxiv* (2022).
28. Flynn, B.I., *et al.* Deep learning based phenotyping of medical images improves power for gene discovery of complex disease. *medRxiv*, 2023.2003. 2007.23286909 (2023).
29. Kun, E., *et al.* The genetic architecture of the human skeletal form. *bioRxiv* (2023).
30. Guo, J., *et al.* Mendelian randomization analyses support causal relationships between brain imaging-derived phenotypes and risk of psychiatric disorders. *Nature Neuroscience* **25**, 1519-1527 (2022).

31. Chen, X.*, et al.* Kidney damage causally affects the brain cortical structure: a Mendelian randomization study. *EBioMedicine* **72**, 103592 (2021).
32. Williams, J.A.*, et al.* Inflammation and brain structure in schizophrenia and other neuropsychiatric disorders: a Mendelian randomization study. *JAMA psychiatry* **79**, 498-507 (2022).
33. Topiwala, A.*, et al.* Associations between moderate alcohol consumption, brain iron, and cognition in UK Biobank participants: observational and mendelian randomization analyses. *PLoS medicine* **19**, e1004039 (2022).
34. Holmes, M.V.*, et al.* Mendelian randomization of blood lipids for coronary heart disease. *European heart journal* **36**, 539-550 (2015).
35. Lamina, C. & Kronenberg, F. Estimation of the required lipoprotein (a)-lowering therapeutic effect size for reduction in coronary heart disease outcomes: a Mendelian randomization analysis. *JAMA cardiology* **4**, 575-579 (2019).
36. Sudlow, C.*, et al.* UK biobank: an open access resource for identifying the causes of a wide range of complex diseases of middle and old age. *PLoS medicine* **12**, e1001779 (2015).
37. Bijsterbosch, J.*, et al.* Investigations into within-and between-subject resting-state amplitude variations. *Neuroimage* **159**, 57-69 (2017).
38. Bai, W.*, et al.* A population-based phenome-wide association study of cardiac and aortic structure and function. *Nature Medicine* **26**, 1654-1662 (2020).
39. Zhao, B.*, et al.* Heart-brain connections: phenotypic and genetic insights from magnetic resonance images. *Science*, just-accepted (2023).
40. Bowden, J.*, et al.* A framework for the investigation of pleiotropy in two-sample summary data Mendelian randomization. *Statistics in medicine* **36**, 1783-1802 (2017).
41. Burgess, S., Butterworth, A. & Thompson, S.G. Mendelian randomization analysis with multiple genetic variants using summarized data. *Genetic epidemiology* **37**, 658-665 (2013).
42. Bowden, J.*, et al.* Improving the accuracy of two-sample summary-data Mendelian randomization: moving beyond the NOME assumption. *Int J Epidemiol* **48**, 728-742 (2019).

43. Bowden, J., Davey Smith, G. & Burgess, S. Mendelian randomization with invalid instruments: effect estimation and bias detection through Egger regression. *International journal of epidemiology* **44**, 512-525 (2015).
44. Hartwig, F.P., Davey Smith, G. & Bowden, J. Robust inference in summary data Mendelian randomization via the zero modal pleiotropy assumption. *International journal of epidemiology* **46**, 1985-1998 (2017).
45. Bowden, J., Davey Smith, G., Haycock, P.C. & Burgess, S. Consistent estimation in Mendelian randomization with some invalid instruments using a weighted median estimator. *Genetic epidemiology* **40**, 304-314 (2016).
46. Ye, T., Shao, J. & Kang, H. Debiased inverse-variance weighted estimator in two-sample summary-data Mendelian randomization. *The Annals of statistics* **49**, 2079-2100 (2021).
47. Zhao, Q., Wang, J., Hemani, G., Bowden, J. & Small, D.S. Statistical inference in two-sample summary-data Mendelian randomization using robust adjusted profile score. *The Annals of Statistics* **48**, 1742-1769 (2020).
48. Wang, J.*, et al.* Causal inference for heritable phenotypic risk factors using heterogeneous genetic instruments. *PLoS genetics* **17**, e1009575 (2021).
49. Oishi, K., Mielke, M.M., Albert, M., Lyketsos, C.G. & Mori, S. DTI analyses and clinical applications in Alzheimer's disease. *J Alzheimers Dis* **26 Suppl 3**, 287-296 (2011).
50. Yin, R.-H.*, et al.* Multimodal voxel-based meta-analysis of white matter abnormalities in Alzheimer's disease. *Journal of Alzheimer's Disease* **47**, 495-507 (2015).
51. Li, R.*, et al.* Attention-related networks in Alzheimer's disease: A resting functional MRI study. *Human brain mapping* **33**, 1076-1088 (2012).
52. Stratos, C., Stefanadis, C., Kallikazaros, I., Boudoulas, H. & Toutouzas, P. Ascending aorta distensibility abnormalities in hypertensive patients and response to nifedipine administration. *The American journal of medicine* **93**, 505-512 (1992).
53. Asmar, R.*, et al.* Aortic distensibility in normotensive, untreated and treated hypertensive patients. *Blood pressure* **4**, 48-54 (1995).

54. Nabati, M., Namazi, S.S., Yazdani, J. & Sharif Nia, H. Relation between aortic stiffness index and distensibility with age in hypertensive patients. *International journal of general medicine*, 297-303 (2020).
55. Lembo, M.*, et al.* Advanced imaging tools for evaluating cardiac morphological and functional impairment in hypertensive disease. *Journal of Hypertension* **40**, 4-14 (2022).
56. Di Palo, K.E. & Barone, N.J. Hypertension and heart failure: prevention, targets, and treatment. *Heart failure clinics* **16**, 99-106 (2020).
57. Gopinathannair, R.*, et al.* Managing atrial fibrillation in patients with heart failure and reduced ejection fraction: a scientific statement from the American Heart Association. *Circulation: Arrhythmia and Electrophysiology* **14**, e000078 (2021).
58. Packer, M. Do most patients with obesity or type 2 diabetes, and atrial fibrillation, also have undiagnosed heart failure? A critical conceptual framework for understanding mechanisms and improving diagnosis and treatment. *European journal of heart failure* **22**, 214-227 (2020).
59. Fujikura, K.*, et al.* Aortic enlargement in chronic obstructive pulmonary disease (COPD) and emphysema: The Multi-Ethnic Study of Atherosclerosis (MESA) COPD study. *Int J Cardiol* **331**, 214-220 (2021).
60. Maclay, J.D.*, et al.* Systemic elastin degradation in chronic obstructive pulmonary disease. *Thorax* **67**, 606-612 (2012).
61. Berman, M.N., Tupper, C. & Bhardwaj, A. Physiology, Left Ventricular Function. (2019).
62. Kim, D.-Y. & Camilleri, M. Serotonin: a mediator of the brain–gut connection. *Official journal of the American College of Gastroenterology| ACG* **95**, 2698-2709 (2000).
63. Jones, M., Dilley, J., Drossman, D. & Crowell, M. Brain–gut connections in functional GI disorders: anatomic and physiologic relationships. *Neurogastroenterology & Motility* **18**, 91-103 (2006).
64. Keefer, L.*, et al.* A Rome working team report on brain-gut behavior therapies for disorders of gut-brain interaction. *Gastroenterology* **162**, 300-315 (2022).
65. Xie, Z., Tong, S., Chu, X., Feng, T. & Geng, M. Chronic kidney disease and cognitive impairment: The kidney-brain axis. *Kidney Diseases* **8**, 275-285 (2022).

66. de Donato, A., Buonincontri, V., Borriello, G., Martinelli, G. & Mone, P. The dopamine system: insights between kidney and brain. *Kidney and Blood Pressure Research* **47**, 493-505 (2022).
67. McCracken, C.*, et al.* Multi-organ imaging demonstrates the heart-brain-liver axis in UK Biobank participants. *Nature Communications* **13**, 7839 (2022).
68. Voulgaris, A., Marrone, O., Bonsignore, M.R. & Steiropoulos, P. Chronic kidney disease in patients with obstructive sleep apnea. A narrative review. *Sleep Medicine Reviews* **47**, 74-89 (2019).
69. Sim, J.J., Rasgon, S.A. & Derose, S.F. Managing sleep apnoea in kidney diseases. *Nephrology* **15**, 146-152 (2010).
70. O'Reilly, R.A. Splenomegaly in 2,505 patients in a large university medical center from 1913 to 1995. 1913 to 1962: 2,056 patients. *Western journal of medicine* **169**, 78 (1998).
71. Vinchi, F.*, et al.* Atherosclerosis is aggravated by iron overload and ameliorated by dietary and pharmacological iron restriction. *European heart journal* **41**, 2681-2695 (2020).
72. Kempf, T. & Wollert, K.C. Iron and atherosclerosis: too much of a good thing can be bad. *European Heart Journal* (2020).
73. Balint, G.P. & Balint, P.V. Felty's syndrome. *Best practice & research clinical rheumatology* **18**, 631-645 (2004).
74. Blendis, L., Ansell, I., Jones, K.L., Hamilton, E. & Williams, R. Liver in Felty's syndrome. *Br Med J* **1**, 131-135 (1970).
75. Kataria, Y.P. & Whitcomb, M.E. Splenomegaly in sarcoidosis. *Archives of Internal Medicine* **140**, 35-37 (1980).
76. Candia, L., Marquez, J. & Espinoza, L.R. Autoimmune hepatitis and pregnancy: a rheumatologist's dilemma. in *Seminars in arthritis and rheumatism*, Vol. 35 49-56 (Elsevier, 2005).
77. Wang, Z.*, et al.* Iron drives T helper cell pathogenicity by promoting RNA-binding protein PCBP1-mediated proinflammatory cytokine production. *Immunity* **49**, 80-92. e87 (2018).
78. Erie, J.C.*, et al.* Heavy metal concentrations in human eyes. *American journal of ophthalmology* **139**, 888-893 (2005).

79. Honka, H.*, et al.* The effects of bariatric surgery on pancreatic lipid metabolism and blood flow. *The Journal of Clinical Endocrinology & Metabolism* **100**, 2015-2023 (2015).
80. Huang, J.-A., Lin, C.-H., Chang, Y.-T., Lee, C.-T. & Wu, M.-J. Nephrotic syndrome is associated with increased risk of ischemic stroke. *Journal of Stroke and Cerebrovascular Diseases* **28**, 104322 (2019).
81. Gigante, A.*, et al.* Nephrotic syndrome and stroke. *International Journal of Immunopathology and Pharmacology* **26**, 769-772 (2013).
82. Roy, C.*, et al.* Ischemic stroke of possible embolic etiology associated with nephrotic syndrome. *Kidney International Reports* **2**, 988-994 (2017).
83. Cheon, S.Y. & Song, J. Novel insights into non-alcoholic fatty liver disease and dementia: insulin resistance, hyperammonemia, gut dysbiosis, vascular impairment, and inflammation. *Cell & Bioscience* **12**, 1-14 (2022).
84. Rodrigo, R.*, et al.* Hyperammonemia induces neuroinflammation that contributes to cognitive impairment in rats with hepatic encephalopathy. *Gastroenterology* **139**, 675-684 (2010).
85. Rose, C.F.*, et al.* Hepatic encephalopathy: Novel insights into classification, pathophysiology and therapy. *Journal of hepatology* **73**, 1526-1547 (2020).
86. Kong, S.H., Park, Y.J., Lee, J.-Y., Cho, N.H. & Moon, M.K. Insulin resistance is associated with cognitive decline among older Koreans with normal baseline cognitive function: a prospective community-based cohort study. *Scientific reports* **8**, 650 (2018).
87. Hobson-Webb, L.D., Massey, J.M., Juel, V.C. & Sanders, D.B. The ultrasonographic wrist-to-forearm median nerve area ratio in carpal tunnel syndrome. *Clinical neurophysiology* **119**, 1353-1357 (2008).
88. Paluch, Ł., Pietruski, P., Walecki, J. & Noszczyk, B.H. Wrist to forearm ratio as a median nerve shear wave elastography test in carpal tunnel syndrome diagnosis. *Journal of Plastic, Reconstructive & Aesthetic Surgery* **71**, 1146-1152 (2018).
89. Gotsopoulos, H., Chen, C., Qian, J. & Cistulli, P.A. Oral appliance therapy improves symptoms in obstructive sleep apnea: a randomized, controlled trial. *American journal of respiratory and critical care medicine* **166**, 743-748 (2002).

90. Araie, T., Okuno, K., Minagi, H.O. & Sakai, T. Dental and skeletal changes associated with long-term oral appliance use for obstructive sleep apnea: a systematic review and meta-analysis. *Sleep Medicine Reviews* **41**, 161-172 (2018).
91. Sander, J.E. & Sharp, F.R. Lumbosacral plexus neuritis. *Neurology* **31**, 470-473 (1981).
92. Khamis, S. & Carmeli, E. A new concept for measuring leg length discrepancy. *Journal of orthopaedics* **14**, 276-280 (2017).
93. Raczkowski, J.W., Daniszewska, B. & Zolynski, K. Functional scoliosis caused by leg length discrepancy. *Archives of Medical Science* **6**, 393-398 (2010).
94. Nelson, C.P.*, et al.* Genetically determined height and coronary artery disease. *New England Journal of Medicine* **372**, 1608-1618 (2015).
95. Schmidt, M., Bøtker, H.E., Pedersen, L. & Sørensen, H.T. Adult height and risk of ischemic heart disease, atrial fibrillation, stroke, venous thromboembolism, and premature death: a population based 36-year follow-up study. *European journal of epidemiology* **29**, 111-118 (2014).
96. Yin, F., Spurgeon, H.A., Rakusan, K., Weisfeldt, M.L. & Lakatta, E.G. Use of tibial length to quantify cardiac hypertrophy: application in the aging rat. *American Journal of Physiology-Heart and Circulatory Physiology* **243**, H941-H947 (1982).
97. Walker, V.M., Zheng, J., Gaunt, T.R. & Smith, G.D. Phenotypic Causal Inference Using Genome-Wide Association Study Data: Mendelian Randomization and Beyond. *Annu Rev Biomed Data Sci* **5**, 1-17 (2022).
98. Burgess, S., Davies, N.M. & Thompson, S.G. Bias due to participant overlap in two-sample Mendelian randomization. *Genetic epidemiology* **40**, 597-608 (2016).
99. Berridge, K.C. & Kringelbach, M.L. Pleasure systems in the brain. *Neuron* **86**, 646-664 (2015).
100. Bressler, S.L. & Menon, V. Large-scale brain networks in cognition: emerging methods and principles. *Trends Cogn Sci* **14**, 277-290 (2010).
101. Wang, K.*, et al.* Altered functional connectivity in early Alzheimer's disease: A resting-state fMRI study. *Human brain mapping* **28**, 967-978 (2007).

102. Sorg, C., *et al.* Selective changes of resting-state networks in individuals at risk for Alzheimer's disease. *Proceedings of the National Academy of Sciences* **104**, 18760-18765 (2007).

103. Ranasinghe, K.G., *et al.* Regional functional connectivity predicts distinct cognitive impairments in Alzheimer's disease spectrum. *NeuroImage: Clinical* **5**, 385-395 (2014).

104. Pini, L., *et al.* A low-dimensional cognitive-network space in Alzheimer's disease and frontotemporal dementia. *Alzheimer's Research & Therapy* **14**, 199 (2022).

105. Liu, W., *et al.* Brain–heart communication in health and diseases. *Brain Research Bulletin* (2022).

106. Walker, K.A., Power, M.C. & Gottesman, R.F. Defining the relationship between hypertension, cognitive decline, and dementia: a review. *Current hypertension reports* **19**, 1-16 (2017).

107. Zhang, H., *et al.* Reduced regional gray matter volume in patients with chronic obstructive pulmonary disease: a voxel-based morphometry study. *American Journal of Neuroradiology* **34**, 334-339 (2013).

108. do Carmo, J.M., *et al.* Role of the brain melanocortins in blood pressure regulation. *Biochimica et Biophysica Acta (BBA)-Molecular Basis of Disease* **1863**, 2508-2514 (2017).

109. Goriely, A., *et al.* Mechanics of the brain: perspectives, challenges, and opportunities. *Biomechanics and modeling in mechanobiology* **14**, 931-965 (2015).

110. Polkey, M.I., Lyall, R.A., Moxham, J. & Leigh, P.N. Respiratory aspects of neurological disease. *Journal of Neurology, Neurosurgery & Psychiatry* **66**, 5-15 (1999).

111. Pollock, R.D., Rafferty, G.F., Moxham, J. & Kalra, L. Respiratory muscle strength and training in stroke and neurology: a systematic review. *International Journal of Stroke* **8**, 124-130 (2013).

112. Tian, C., Zhao, J., Xiong, Q., Yu, H. & Du, H. Secondary iron overload induces chronic pancreatitis and ferroptosis of acinar cells in mice. *International Journal of Molecular Medicine* **51**, 1-13 (2023).

113. Galaris, D., Barbouti, A. & Pantopoulos, K. Iron homeostasis and oxidative stress: An intimate relationship. *Biochimica et Biophysica Acta (BBA)-Molecular Cell Research* **1866**, 118535 (2019).
114. Robles, L., Vaziri, N.D. & Ichii, H. Role of oxidative stress in the pathogenesis of pancreatitis: effect of antioxidant therapy. *Pancreatic disorders & therapy* **3**, 112 (2013).
115. Armstrong, J.*, et al.* Oxidative stress in acute pancreatitis: lost in translation? *Free radical research* **47**, 917-933 (2013).
116. Pérez, S., Pereda, J., Sabater, L. & Sastre, J. Redox signaling in acute pancreatitis. *Redox biology* **5**, 1-14 (2015).
117. Kushner, T. & Cafardi, J. Chronic liver disease and COVID-19: alcohol use disorder/alcohol-associated liver disease, nonalcoholic fatty liver disease/nonalcoholic steatohepatitis, autoimmune liver disease, and compensated cirrhosis. *Clinical Liver Disease* **15**, 195 (2020).
118. Grant, I., Heaton, R.K., McSweeney, A.J., Adams, K.M. & Timms, R.M. Brain dysfunction in COPD. *Chest* **77**, 308-309 (1980).
119. Spilling, C.A.*, et al.* Factors affecting brain structure in smoking-related diseases: Chronic Obstructive Pulmonary Disease (COPD) and coronary artery disease. *PLoS One* **16**, e0259375 (2021).
120. Kim, G.A.*, et al.* Association between non-alcoholic fatty liver disease and the risk of dementia: a nationwide cohort study. *Liver international* **42**, 1027-1036 (2022).
121. Kim, D.-G.*, et al.* Non-alcoholic fatty liver disease induces signs of Alzheimer's disease (AD) in wild-type mice and accelerates pathological signs of AD in an AD model. *Journal of neuroinflammation* **13**, 1-18 (2016).
122. Wang, L., Sang, B. & Zheng, Z. Risk of dementia or cognitive impairment in non-alcoholic fatty liver disease: A systematic review and meta-analysis. *Frontiers in Aging Neuroscience* **14**(2022).
123. Mobeen, S. & Apostol, R. Ovarian cyst. (2020).
124. Padda, J.*, et al.* Depression and its effect on the menstrual cycle. *Cureus* **13**(2021).

125. Azari, A.A. & Barney, N.P. Conjunctivitis: a systematic review of diagnosis and treatment. *Jama* **310**, 1721-1730 (2013).
126. Sankowski, R., Mader, S. & Valdés-Ferrer, S.I. Systemic inflammation and the brain: novel roles of genetic, molecular, and environmental cues as drivers of neurodegeneration. *Frontiers in cellular neuroscience* **9**, 28 (2015).
127. Elwood, E., Lim, Z., Naveed, H. & Galea, I. The effect of systemic inflammation on human brain barrier function. *Brain, behavior, and immunity* **62**, 35-40 (2017).
128. Rhyou, H.-I. & Nam, Y.-H. Association between cognitive function and asthma in adults. *Annals of Allergy, Asthma & Immunology* **126**, 69-74 (2021).
129. Ray, M., Sano, M., Wisnivesky, J.P., Wolf, M.S. & Federman, A.D. Asthma control and cognitive function in a cohort of elderly adults. *Journal of the American Geriatrics Society* **63**, 684-691 (2015).
130. Alvarez, J.I., Cayrol, R. & Prat, A. Disruption of central nervous system barriers in multiple sclerosis. *Biochimica et Biophysica Acta (BBA)-Molecular Basis of Disease* **1812**, 252-264 (2011).
131. Krupp, L.B.*, et al.* International Pediatric Multiple Sclerosis Study Group criteria for pediatric multiple sclerosis and immune-mediated central nervous system demyelinating disorders: revisions to the 2007 definitions. *Multiple Sclerosis Journal* **19**, 1261-1267 (2013).
132. Huda, S.*, et al.* Neuromyelitis optica spectrum disorders. *Clinical Medicine* **19**, 169 (2019).
133. Kim, W., Kim, S.-H., Huh, S.-Y. & Kim, H.J. Brain abnormalities in neuromyelitis optica spectrum disorder. *Multiple sclerosis international* **2012**(2012).
134. Lancaster, E. The diagnosis and treatment of autoimmune encephalitis. *Journal of Clinical Neurology* **12**, 1-13 (2016).
135. Wartolowska, K.*, et al.* Structural changes of the brain in rheumatoid arthritis. *Arthritis & Rheumatism* **64**, 371-379 (2012).
136. Kozora, E. & Filley, C.M. Cognitive dysfunction and white matter abnormalities in systemic lupus erythematosus. *Journal of the International Neuropsychological Society* **17**, 385-392 (2011).
137. Appenzeller, S.*, et al.* Longitudinal analysis of gray and white matter loss in patients with systemic lupus erythematosus. *Neuroimage* **34**, 694-701 (2007).

138. Rosenberg, G.A. Inflammation and white matter damage in vascular cognitive impairment. *Stroke* **40**, S20-S23 (2009).
139. Raj, D.*, et al.* Increased white matter inflammation in aging-and Alzheimer's disease brain. *Frontiers in molecular neuroscience* **10**, 206 (2017).
140. Gerdts, E.*, et al.* Correlates of left atrial size in hypertensive patients with left ventricular hypertrophy: the Losartan Intervention For Endpoint Reduction in Hypertension (LIFE) Study. *Hypertension* **39**, 739-743 (2002).
141. Eshoo, S., Ross, D.L. & Thomas, L. Impact of mild hypertension on left atrial size and function. *Circulation: Cardiovascular Imaging* **2**, 93-99 (2009).
142. Sanfilippo, A.J.*, et al.* Atrial enlargement as a consequence of atrial fibrillation. A prospective echocardiographic study. *Circulation* **82**, 792-797 (1990).
143. van de Vegte, Y.J., Siland, J.E., Rienstra, M. & van der Harst, P. Atrial fibrillation and left atrial size and function: a Mendelian randomization study. *Scientific reports* **11**, 8431 (2021).
144. Hiraiwa, H.*, et al.* Clinical significance of spleen size in patients with heart failure. *European Heart Journal* **42**, ehab724. 0756 (2021).
145. Ormazabal, V.*, et al.* Association between insulin resistance and the development of cardiovascular disease. *Cardiovascular diabetology* **17**, 1-14 (2018).
146. Shah, A., Mehta, N. & Reilly, M.P. Adipose inflammation, insulin resistance, and cardiovascular disease. *Journal of Parenteral and Enteral Nutrition* **32**, 638-644 (2008).
147. Thurlbeck, W.M. & Müller, N. Emphysema: definition, imaging, and quantification. *AJR. American journal of roentgenology* **163**, 1017-1025 (1994).
148. Fernández-García, V., González-Ramos, S., Martín-Sanz, P., Castrillo, A. & Boscá, L. Contribution of extramedullary hematopoiesis to atherosclerosis. The spleen as a neglected hub of inflammatory cells. *Frontiers in Immunology* **11**, 586527 (2020).
149. Suttorp, M. & Classen, C.F. Splenomegaly in children and adolescents. *Frontiers in pediatrics*, 693 (2021).
150. Lampropoulos, C.E., Papaioannou, I. & D'cruz, D.P. Osteoporosis—a risk factor for cardiovascular disease? *Nature Reviews Rheumatology* **8**, 587-598 (2012).

151. Gaines, J.M., *et al.* Older men's knowledge of osteoporosis and the prevalence of risk factors. *Journal of Clinical Densitometry* **13**, 204-209 (2010).
152. Whalen, R., Carter, D. & Steele, C. Influence of physical activity on the regulation of bone density. *Journal of biomechanics* **21**, 825-837 (1988).
153. Zhao, Q., Wang, J., Spiller, W., Bowden, J. & Small, D.S. Two-sample instrumental variable analyses using heterogeneous samples. *Statistical Science* **34**, 317-333 (2019).
154. Cui, R., *et al.* Improving fine-mapping by modeling infinitesimal effects. *bioRxiv*, 2022.2010. 2021.513123 (2022).
155. Xue, H., Shen, X. & Pan, W. Causal Inference in Transcriptome-Wide Association Studies with Invalid Instruments and GWAS Summary Data. *Journal of the American Statistical Association*, 1-27 (2023).
156. Tseng, W.Y., Su, M.Y. & Tseng, Y.H. Introduction to Cardiovascular Magnetic Resonance: Technical Principles and Clinical Applications. *Acta Cardiol Sin* **32**, 129-144 (2016).
157. Pennell, D.J. Cardiovascular magnetic resonance. *Circulation* **121**, 692-705 (2010).
158. Bai, W., *et al.* Automated cardiovascular magnetic resonance image analysis with fully convolutional networks. *Journal of Cardiovascular Magnetic Resonance* **20**, 1-12 (2018).
159. Bai, W., *et al.* Recurrent neural networks for aortic image sequence segmentation with sparse annotations. *International conference on medical image computing and computer-assisted intervention*, 586-594 (2018).
160. Miller, K.L., *et al.* Multimodal population brain imaging in the UK Biobank prospective epidemiological study. *Nat Neurosci* **19**, 1523-1536 (2016).
161. Zhao, B., *et al.* Heritability of regional brain volumes in large-scale neuroimaging and genetic studies. *Cerebral Cortex* **29**, 2904-2914 (2019).
162. Zhao, B., *et al.* Large-scale GWAS reveals genetic architecture of brain white matter microstructure and genetic overlap with cognitive and mental health traits (n= 17,706). *Molecular psychiatry* **26**, 3943-3955 (2021).
163. Avants, B.B., *et al.* A reproducible evaluation of ANTs similarity metric performance in brain image registration. *Neuroimage* **54**, 2033-2044 (2011).

164. Jahanshad, N., *et al.* Multi-site genetic analysis of diffusion images and voxelwise heritability analysis: A pilot project of the ENIGMA–DTI working group. *Neuroimage* **81**, 455-469 (2013).
165. Kochunov, P., *et al.* Multi-site study of additive genetic effects on fractional anisotropy of cerebral white matter: comparing meta and megaanalytical approaches for data pooling. *Neuroimage* **95**, 136-150 (2014).
166. Glasser, M.F., *et al.* A multi-modal parcellation of human cerebral cortex. *Nature* **536**, 171-178 (2016).
167. Ji, J.L., *et al.* Mapping the human brain's cortical-subcortical functional network organization. *Neuroimage* **185**, 35-57 (2019).
168. Bowden, J., *et al.* Improving the accuracy of two-sample summary-data Mendelian randomization: moving beyond the NOME assumption. *International journal of epidemiology* **48**, 728-742 (2019).

METHODS

Multi-organ imaging biomarkers.

The imaging data were sourced from the UK Biobank (UKB) study, which enrolled approximately 500,000 individuals aged between 40 and 69 from 2006 to 2010 (https://www.ukbiobank.ac.uk/). These multi-organ imaging data were collected from the ongoing UKB imaging study project (https://www.ukbiobank.ac.uk/explore-your-participation/contribute-further/imaging-study), which aims to collect brain, heart, and abdomen scans from 100,000 participants. Ethical approval for the UKB study was secured from the North West Multicentre Research Ethics Committee (approval number: 11/NW/0382).

Studies of brain and heart diseases usually rely on magnetic resonance imaging (MRI) scans, which are well-established clinical endophenotypes. Cardiovascular magnetic resonance imaging (CMR) is a set of MRI techniques that are designed to assess ventricular function, cardiovascular morphology, myocardial perfusion, and other cardiac functional and structural features[156,157]. They have been frequently used to reveal heart-related issues clinically. The CMR traits used in the paper were originally generated from the raw short-axis, long-axis, and aortic cine images using the state-of-the-art heart

imaging segmentation and feature representation framework[38,158,159]. We divided the generated 82 CMR traits into 6 categories. The first two are aortic sections, namely ascending aorta (AAo) and descending aorta (DAo), which serve as the main 'pipe' in supplying blood to the entire body. The other four are the global measures of 4 cardiac chambers, including the left ventricle (LV), right ventricle (RV), left atrium (LA), and right atrium (RA), which altogether manage the heartbeat and blood flow. There are also some other traits, such as regional phenotypes of the left ventricle myocardial-wall thickness and strain (**Table S1**). The summary-level GWAS data of these 82 CMR traits were obtained from Zhao, et al. [39].

Brain MRI provides detailed information about brain structure and function[160], such as abnormal growth, healthy aging, white matter diseases, structural issues, and functional abnormalities. In this paper, the summary-level GWAS data were collected from recent multi-modal image genetic studies, including regional brain volumes from structural MRI[21,161] (sMRI), diffusion tensor imaging (DTI) parameters from diffusion MRI[23,162] (dMRI), and functional activity (that is, amplitude[37]) and functional connectivity phenotypes from resting functional MRI[25] (resting fMRI). In sMRI, we used ANTs[163] to generate regional brain volumes for cortical and subcortical regions and global brain volume measures. In dMRI, we used the ENIGMA-DTI pipelines[164,165] to generate tract-averaged parameters for fractional anisotropy, mean diffusivity, axial diffusivity, radial diffusivity, and mode of anisotropy in major white matter tracts and across the whole brain. For resting fMRI, we extracted phenotypes from brain parcellation-based analysis. We used the Glasser360 atlas[166], which divided the cerebral cortex into 360 regions in 12 functional networks[167]. We considered 90 network-level resting fMRI phenotypes that evaluated interactions and spontaneous neural activity at rest.

The 11 imaging biomarkers from abdominal MRI were derived by Liu., et al[8] using deep learning methods in terms of volume, fat, and iron in several organs and tissues, such as the liver, spleen, kidney, lung, pancreas, and adipose tissue. Skeleton DXA traits, including all long bone lengths as well as hip and shoulder width, were derived by Kun., et al[3] using deep learning methods on whole-body dual-energy X-ray absorptiometry (DXA) images.

All eight skeleton traits have been controlled for height. The heritability of the above imaging biomarkers can be found in **Supplementary Note**.

FinnGen clinical endpoints.

We used 88 clinical endpoints collected by the FinnGen project, which were selected from the R7 release and with more than 10,000 cases for most of the clinical endpoints (https://www.finngen.fi/en/access_results). As for some important diseases, such as Alzheimer's disease, we set the cutoff of the number of cases to be 6,000. The 88 clinical endpoints covered diseases from various categories, namely, mental and behavioral disorders, diseases of the nervous system, diseases of the eye and adnexa, diseases of the genitourinary system, diseases of the circulatory systems, cardiometabolic endpoints, diseases marked as autoimmune origin, rheuma endpoints, interstitial lung diseases, COPD and related endpoints, as well as some unclassified endpoints. The definations can be found at https://risteys.finregistry.fi/. The FinnGen data used in our study was obtained from separate cohorts than those supplying imaging traits, which were derived from the UKB study, thus ensuring there was no sample overlap. Detailed information of these 88 clinical variables can be found in **Table S2**.

Mendelian randomization analysis.

We examined the genetic causal relationships between the 402 imaging traits (101 brain regional volume traits, 110 brain DTI parameters, 90 network-level fMRI phenotypes, 82 CMR traits, 11 abdominal traits, and 8 skeleton DXA traits) and 88 clinical endpoints. Prior to conducting the Mendelian randomization (MR) analysis, we conducted standard preprocessing and quality control procedures. First, we selected genetic variants based on a significance threshold of 5×10^{-8} in the exposure GWAS data. To ensure the independence of the genetic variants used in MR, we implemented LD clumping with a window size of 10,000 and an r^2 threshold of 0.01, using the 1000 Genomes European ancestry data as a reference panel. We used the TwoSampleMR package (https://mrcieu.github.io/TwoSampleMR/) for harmonization, which enabled us to accurately align alleles between the selected variants in the exposure and the reported effect on the outcome.

We assessed the performance of 8 MR methods, which included Inverse variance weighted (fixed effect), Inverse variance weighted (multiplicative random effect), MR-Egger, Simple Median, Weighted Median, Weighted Mode, DIVW, GRAPPLE, and MR-RAPS[40,41,43-48,168], where MR Egger was used as the pleiotropy test. To ensure the reliability of our results, we implemented several quality control procedures. We excluded causal estimates that relied on fewer than 6 genetic variants, as a larger number of genetic variants increases the statistical power of MR analysis[46,47]. We retained causal pairs that were significant in at least two out of the eight methods. We also screened for pleiotropy by using the MR-Egger intercept, the most used method for testing the pleiotropy assumption. If a causal estimate failed the MR-Egger intercept test, we required that it have significant results in at least one of the robust MR methods, such as Weighted Median, Weighted Model, MR-RAPS, or GRAPPLE. Out of 488 significant findings, 81 causal estimates failed the MR-Egger intercept test. However, when we interpreted the results, we focused on the ones that passed the MR-Egger intercept test.

Code availability

We made use of publicly available software and tools. Our analysis code will be made freely available at Zenodo.

Data availability

We used summary-level GWAS data in this study, which can be obtained from the FinnGen project (https://www.finngen.fi/en/access_results), BIG-KP (https://bigkp.org/), Heart-KP (https://heartkp.org/), and project-specific resources detailed in Liu., et al[8] and Kun., et al[3]. Our multi-organ MR results can be explored at https://mr4mo.org/.

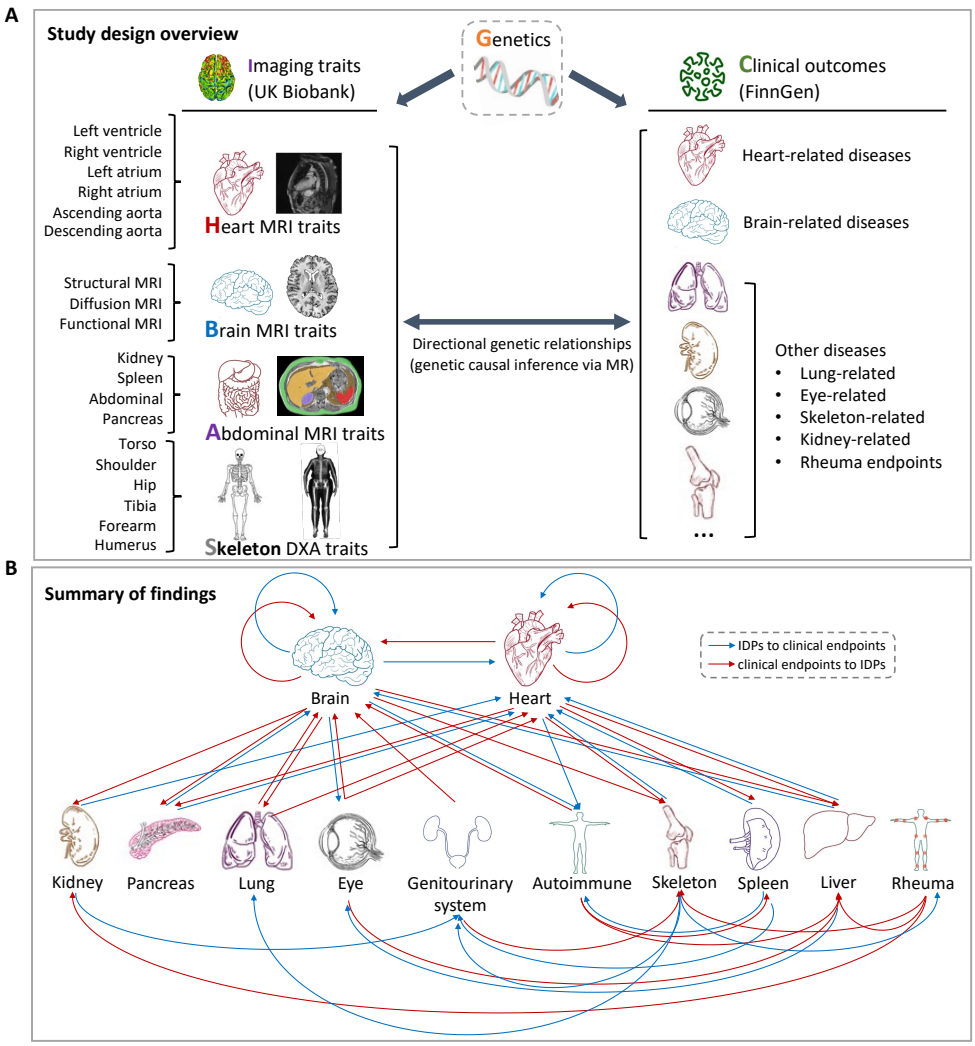

Fig. 1 Overview of study design and findings.

(**A**). An overview of our multi-organ imaging genetic study for 88 clinical outcomes. Multi-modal brain imaging traits, cardiac imaging traits, abdominal imaging traits, as well as skeleton DXA imaging traits were used to investigate the relationship between 88 clinical endpoints. We covered a full spectrum of brain imaging modalities, including structural MRI, diffusion MRI, and resting fMRI. Cardiac imaging data were composed of short-axis, long-axis, and aortic cine images. Volume, iron content, and percent fat were measured in 6 different abdominal organs and tissues, resulting in 11 image-derived abdominal phenotypes. We have 8 skeleton imaging traits that covered long bone lengths as well as hip and shoulder width. (**B**). A high-level summary of our bidirectional findings. IDPs, imaging derived phenotypes.

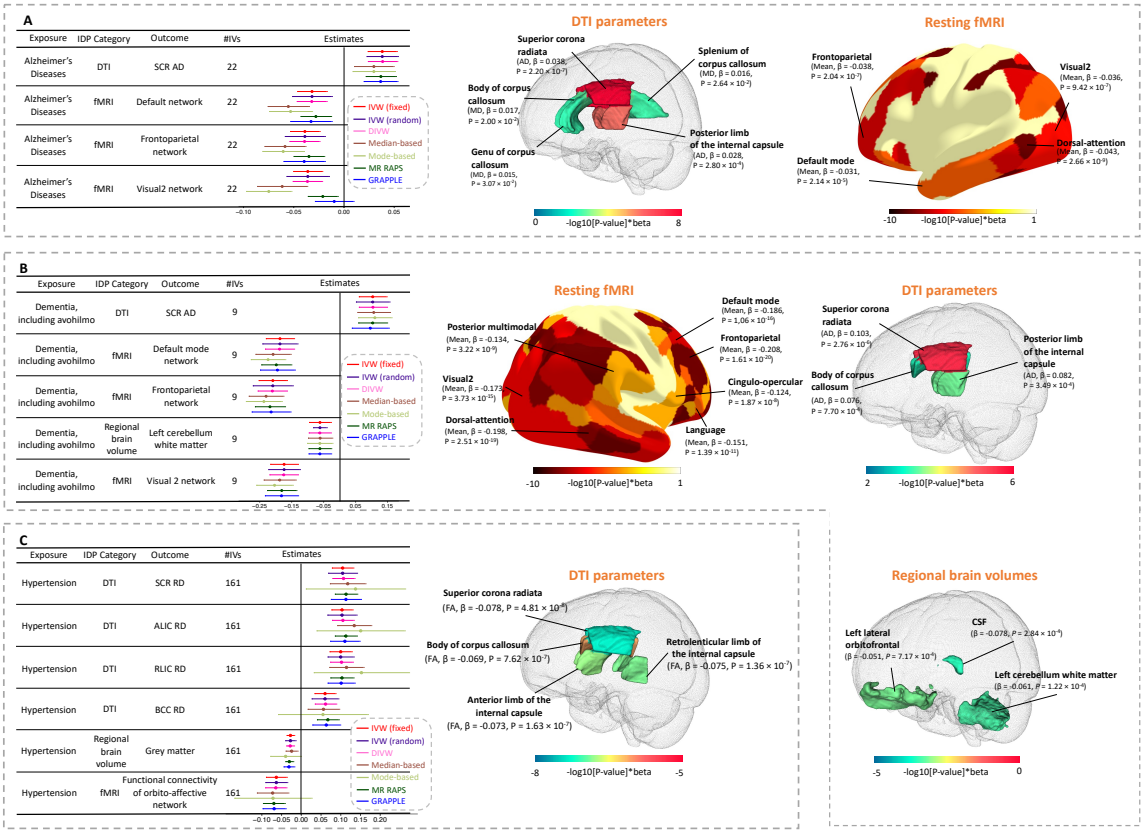

Fig. 2 Selected genetic causal effects of clinical outcomes on brain imaging biomarkers. We illustrated selected significant ($P < 5.18\times10^{-6}$) causal genetic links from clinical endpoints (Exposure) to brain imaging biomarkers (Outcome) after adjusting for multiple testing using the Bonferroni procedure. (**A**). The causal effect of Alzheimer's disease on brain imaging biomarkers. (**B**). The causal effect of dementia on brain imaging biomarkers. (**C**). The causal effect of hypertension on brain imaging biomarkers. IDP Category, category of imaging biomarkers; #IVs, the number of genetic variants used as instrumental variables. Different MR methods and their regression coefficients are labeled with different colors. See **Table S1** for data resources of clinical endpoints and **Table S2** for data resources of imaging biomarkers.

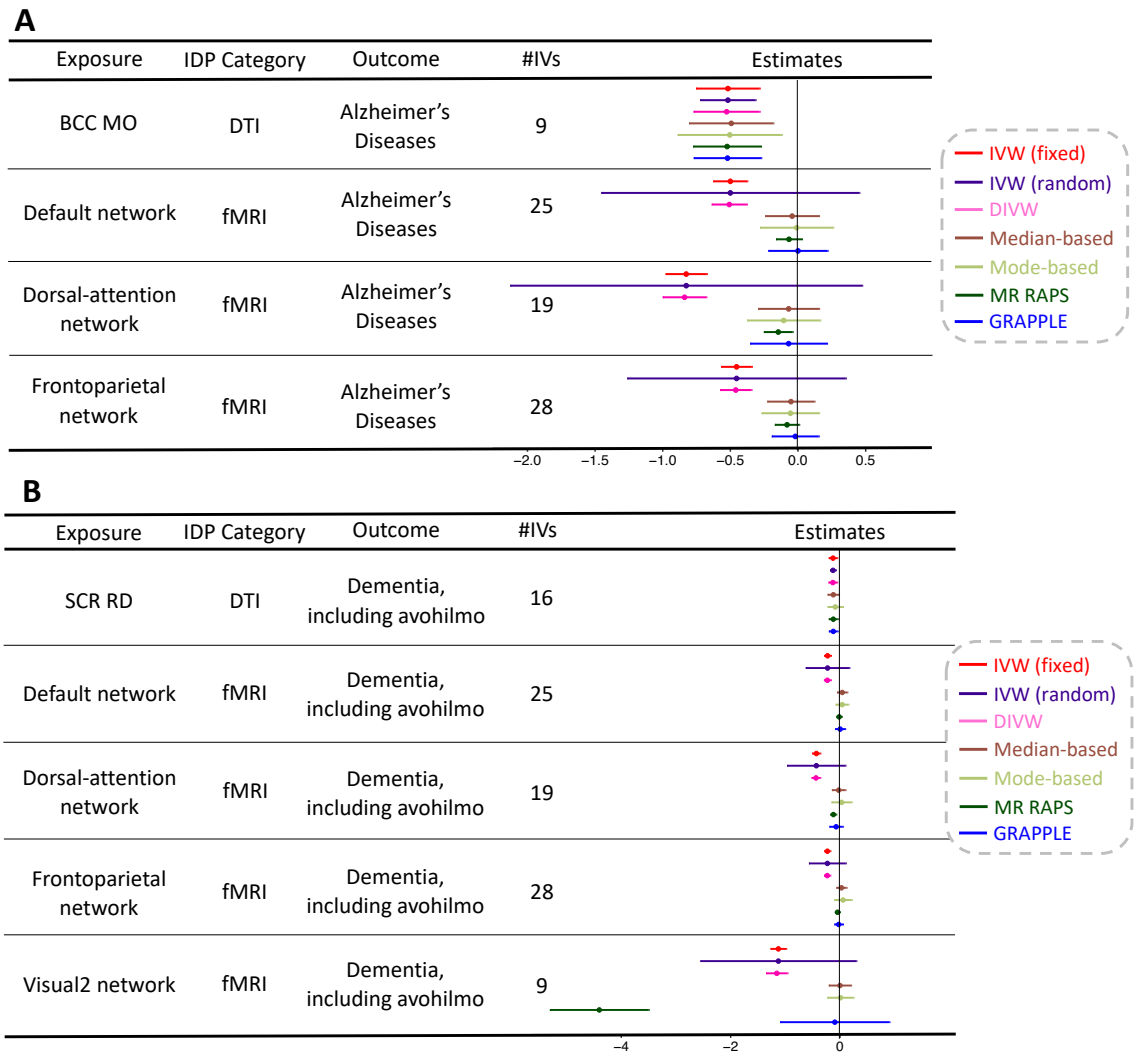

Fig. 3 Selected genetic causal effects of brain imaging biomarkers on clinical endpoints. We illustrated selected significant ($P < 5.18\times10^{-6}$) causal genetic links from brain imaging biomarkers (Exposure) to clinical endpoints (Outcome) after adjusting for multiple testing using the Bonferroni procedure. (**A**). The causal effect of brain imaging biomarkers on Alzheimer's diseases. (**B**). The causal effect of brain imaging biomarkers on dementia. IDP Category, category of imaging biomarkers; #IVs, the number of genetic variants used as instrumental variables. Different MR methods and their regression coefficients are labeled with different colors. See **Table S1** for data resources of clinical endpoints and **Table S2** for data resources of imaging biomarkers.

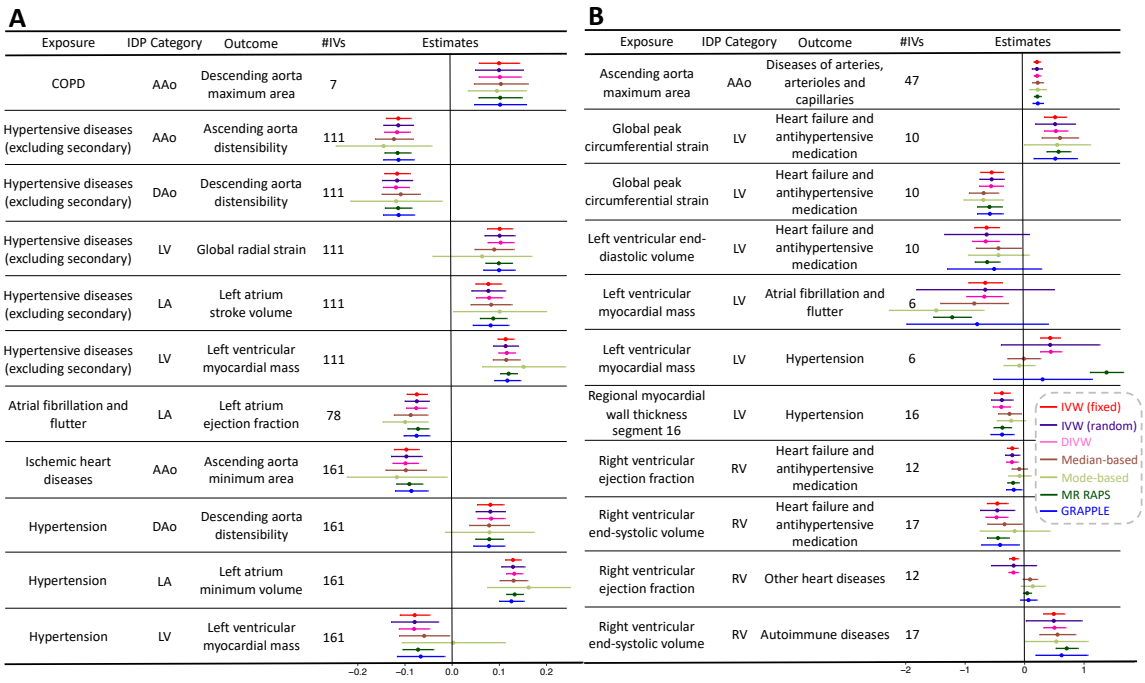

Fig. 4 Selected genetic causal effects between heart imaging biomarkers and clinical endpoints.

We illustrated selected significant ($P < 6.85\times10^{-6}$) causal genetic links from (**A**) clinical endpoints (Exposure) to heart imaging biomarkers (Outcome) and (**B**) heart imaging biomarkers (Exposure) to clinical endpoints (Outcome) after adjusting for multiple testing using the Bonferroni procedure. IDP Category, category of imaging biomarkers; #IVs, the number of genetic variants used as instrumental variables. Different MR methods and their regression coefficients are labeled with different colors. See **Table S1** for data resources of clinical endpoints and **Table S2** for data resources of imaging biomarkers.

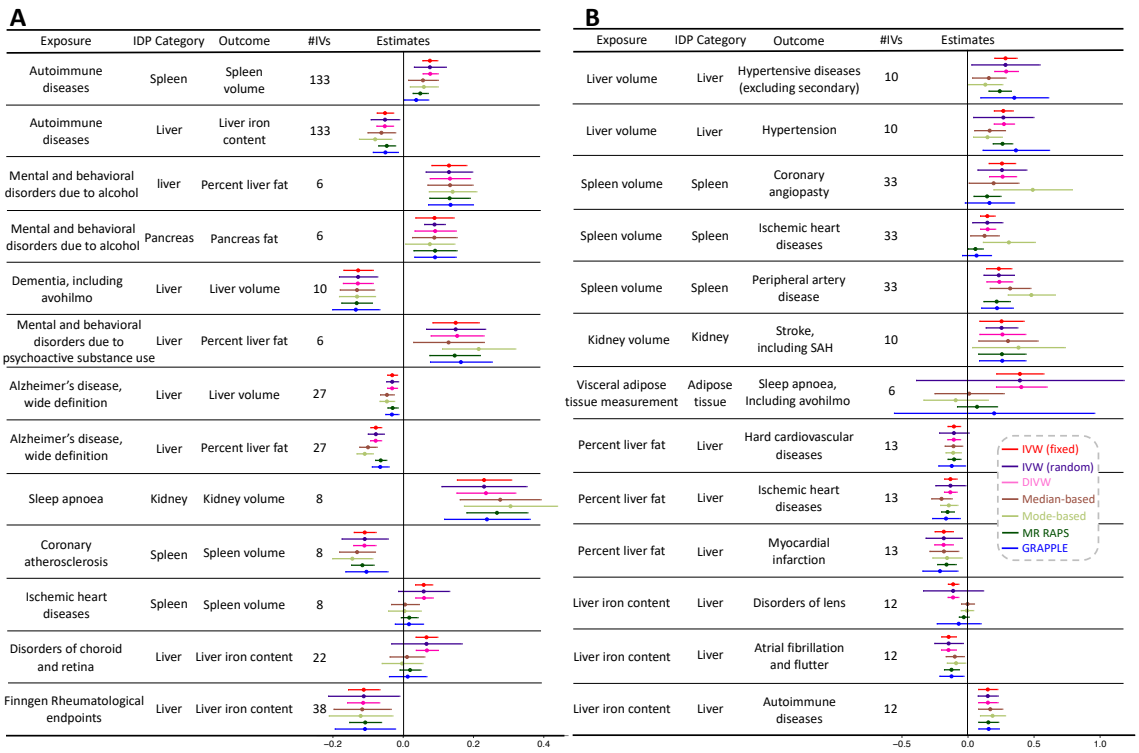

Fig. 5 Selected genetic causal effects between abdominal imaging biomarkers and clinical endpoints.

We illustrated selected significant ($P < 6.69\times10^{-5}$) causal genetic links from (**A**) clinical endpoints (Exposure) to abdominal imaging biomarkers (Outcome) and (**B**) abdominal imaging biomarkers (Exposure) to clinical endpoints (Outcome) after adjusting for multiple testing using the Bonferroni procedure. IDP Category, category of imaging biomarkers; #IVs, the number of genetic variants used as instrumental variables. Different MR methods and their regression coefficients are labeled with different colors. See **Table S1** for data resources of clinical endpoints and **Table S2** for data resources of imaging biomarkers.

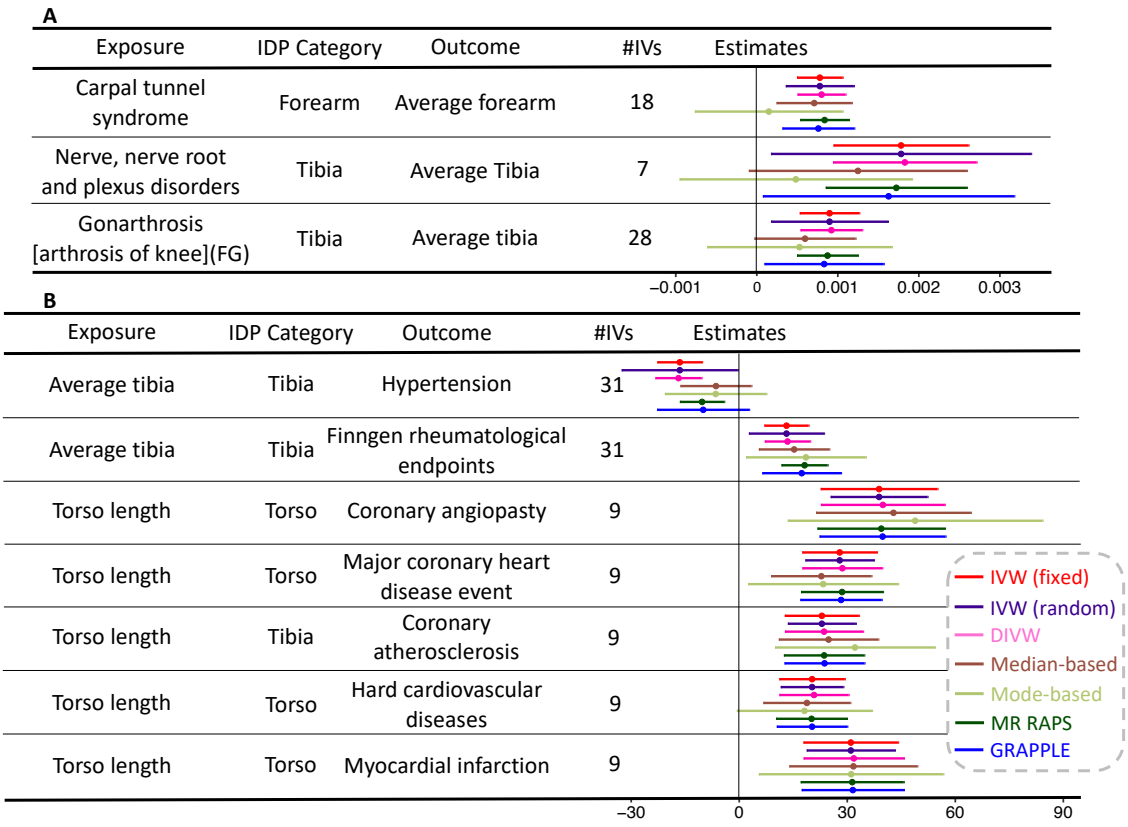

Fig. 6 Selected genetic causal effects between skeleton imaging biomarkers and clinical endpoints.

We illustrated selected significant ($P < 3.39\times10^{-5}$) causal genetic links from (**A**) clinical endpoints to (Exposure) to skeleton imaging biomarkers (Outcome) and (**B**) skeleton imaging biomarkers (Exposure) to clinical endpoints (Outcome) after adjusting for multiple testing using the Bonferroni procedure. IDP Category, category of imaging biomarkers; #IVs, the number of genetic variants used as instrumental variables. Different MR methods and their regression coefficients are labeled with different colors. See **Table S1** for data resources of clinical endpoints and **Table S2** for data resources of imaging biomarkers.